Biomimetic Branched Hollow Fibers Templated by Self-Assembled Fibrous Polyvinylpyrrolidone Structures in Aqueous Solution

Penghe Qiu and Chuanbin Mao*

Department of Chemistry and Biochemistry, University of Oklahoma, 620 Parrington Oval, Room 208, Norman, Oklahoma 73019

ABSTRACT Branched hollow fibers are common in nature, but to form artificial fibers with a similar branched hollow structure is still a challenge. We discovered that polyvinylpyrrolidone (PVP) could self-assemble into branched hollow fibers in an aqueous solution after aging the PVP solution for about two weeks. On the basis of this finding, we demonstrated two approaches by which the self-assembly of PVP into branched hollow fibers could be exploited to template the formation of branched hollow inorganic fibers. First, inorganic material such as silica with high affinity against the PVP could be deposited on the surface of the branched hollow PVP fibers to form branched hollow silica fibers. To extend the application of PVP self-assembly in templating the formation of hollow branched fibers, we then adopted a second approach where the PVP molecules bound to inorganic nanoparticles (using gold nanoparticles as a model) co-self-assemble with the free PVP molecules in an aqueous solution, resulting in the formation of the branched hollow fibers with the nanoparticles embedded in the PVP matrix constituting the walls of the fibers. Heating the resultant fibers above the glass transition temperature of PVP led to the formation of branched hollow gold fibers. Our work suggests that the self-assembly of the PVP molecules in the solution can serve as a general method for directing the formation of branched hollow inorganic fibers. The branched hollow fibers may find potential applications in microfluidics, artificial blood vessel generation, and tissue engineering.

KEYWORDS: branched hollow fibers · polyvinylpyrrolidone · self-assembly · silica · gold · nanoparticles

Branched hollow fibers can be found in nature and play a significant role in the functioning of biological bodies. For example, as the most important vessels, capillaries in the blood vessel system own an abundance of branches, which enable the exchange of chemicals and water between the blood and body tissues. Without the bronchial tree in the respiration system, oxygen transportation will be extremely slow and any intensive body movement will need great effort or even become impossible. Branched hollow fibers are also adopted by many types of birds in their feathers.[1,2] The branched structure of feathers can reduce the weight and increase the friction with air, and also act as a thermal insulator.[2] Mimicking unique branched hollow structures in nature will help us to produce novel advanced materials that can find potential technological and medical applications such as microfluidics,[3] artificial blood vessel generation,[4,5] and lung tissue engineering.[6,7] However, synthesis of branched hollow fibers remains a challenge up to date. Nonbranched solid and hollow fibers of many types of materials have been prepared in different ways, such as chemical vapor deposition (CVD),[8−10] anodic aluminum oxide (AAO) templating,[11] electrospinning,[12,13] and many other wet chemical synthetic methods.[14] So far, branched hollow fibers were only reported in the fabrication of carbon nanotubes[15,16] and polyaniline nanotubes.[17] The branched carbon nanotubes were prepared by directly templating Y-branched nanochannel alumina using CVD, and self-assembled doped polyaniline was formed from the fusion of micelles containing polyaniline and dopants.

The polymer polyvinylpyrrolidone (PVP) has found its application in many scientific areas. For example, in adhesive industry, PVP offers a unique combination of desired properties including good initial tack, transparency, chemical and biological inertness, and very low toxicity. In material science, PVP has acted as a key factor in the shape controlled synthesis of silver and platinum nanocrystals.[18−20] For the synthesis of these nanomaterials, PVP serves as a polymeric capping agent, which can selectively interact with the {100} facets of Ag and Pt, and shape control was realized through the preferential adsorption of atoms onto poorly protected facets such as {111}.[21] PVP has also been widely used as an additive to manipulate solution

*Address correspondence to cbmao@ou.edu.

Received for review May 13, 2009 and accepted February 04, 2010.

Published online February 16, 2010. 10.1021/nn9009196

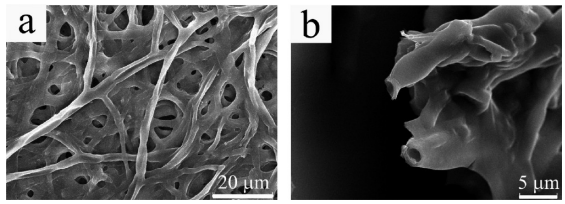

Figure 1. SEM images of self-assembled hollow branched PVP fibers: (a) an aggregate of branched fibers that may be collapsed upon drying on substrate; (b) higher magnification image of the tips of the fibers, showing the hollow nature of the fibers.

viscosity in the production of nanofibers through electrospinning.[12] In addition, in the fabrication of various membrane products, PVP is added to increase the hydrophilicity of the membranes.[22−25] In this work, we discovered that, after a relatively long period of aging at room temperature, PVP could self-assemble to form a macroscopic matrix made of a branched hollow polymer fibers in an aqueous solution. By directly templating the silica formation on the self-assembled fibrous network, branched hollow silica fibers were synthesized. Inspired from the self-assembly of PVP into fibrous structures in the solution, we also studied the self-assembly of PVP-coated nanoparticles into branched fibers. We believe that the self-assembled fibrous PVP structures could be potentially used as a universal template for preparing branched hollow fibers through the synergistic assembly of nanoparticles and PVP in the solution phase.

RESULTS AND DISCUSSIONS

The self-assembled fibrous PVP structure formed in the aqueous solution was a jellyfish-like three-dimensional aggregate with a centimeter scale (Supporting Informaiton, Figure S1-a). However, when taken out of the solution, the aggregate was collapsed immediately into a semitransparent thin film. The SEM imaging of the film revealed that the aggregate was constructed from a network of branched hollow PVP fibers of micrometer size (Figure 1a). The collapsed morphology indicated that the fibers formed might be hollow when in the solution. A closer look at the ends of the polymer fibers shows that the fibers are indeed hollow (Figure 1b). The hollow nature of the PVP fibers was also proved by TEM imaging (Supporting Information, Figure S2). To the best of our knowledge, the self-assembled fibrous structure resulting from the self-assembly of PVP in the aqueous solution has never been reported, although it was not a surprise to us that PVP could self-assemble to form this kind of structure.

The association behavior of polymers in a solution phase has been extensively studied for decades. Generally, van de Waals force and hydrophobic and electrostatic interactions as well as hydrogen bonding are the major driving forces responsible for inter- and intramolecular interaction among polymer molecules.[26] In PVP, both the polymer backbone and methylene groups in the five-member ring provide good sites for hydrophobic interaction, enabling the association of PVP through hydrophobic interaction. In addition, polymer chains with highly electronegative amide groups could be strongly linked together through solvent-mediated H-bonding interaction.[26,27] Earlier, an aggregate of around 100 nm nanoparticles was found to form in a freshly prepared PVP aqueous solution by dynamic light scattering (DLS); however, the detailed structure of the aggregate was not mentioned.[28] Actually, not only PVP, but also other amide containing polymers, such as poly(*N*,*N*-diethylacrylamide) (PDEA), could self-assemble to form aggregates, due to their structural similarity.[29]

We believe that the macroscopic PVP structures shown in Figure 1 result from a self-assembly process in which individual polymer chains interact with each other through H-bonding and hydrophobic interaction. To prove this mechanism, we suspended the polymer aggregates into 1 M urea aqueous solution, which is a common reagent used to break H-bonding in protein science. After one week, we observed a dramatic decrease in the dimension of polymer aggregates, indicating that some polymer chains had been disassembled from the major aggregated structures due to the loss of H-bonding interactions. More detailed mechanism was analyzed by a combination of DLS measurement and SEM imaging.

By using DLS to measure the size distribution of the particles formed during the aging of the aqueous PVP solution, we found that even in the freshly prepared PVP solution, there were particles ranging from 40−80 nm (Supporting Information, Figure S3). Given that the individual polymer chain length (MW = 10 kDa, 91 monomers) should be less than 15 nm, the nanoparticles detected by DLS must be generated from the association of polymer chains. However, after 1 and 4 days, the particle size was increased to 90−160 and 210−490 nm, respectively (Supporting Information, Figure S3). These facts indicate that the polymer molecules gradually self-assemble into larger particles in the solution. At day 6, the PVP aggregates became visible by naked eyes at the bottom of the vial (around 1 mm in diameter). We further examined the tiny aggregates by SEM (Figure 2). It could be seen clearly that in the center of the aggregates there was a core made of chains of PVP microspheres, from which polymer fibers were grown and stretched toward all directions (Figure 2a). A closer look at the core reveals that hollow microspheres are fused into the chains (Figure 2b,c). Longer hollow fibers (Figure 1) were grown from the microspheres at the end of such chains (Figure 2d).

On the basis of the DLS and SEM analysis of the early stage during the formation of the jellyfish-like PVP aggregate, the aggregate formation process can be divided into two steps: formation and fusion of PVP

microspheres into pearl-necklace-like chains and growth of hollow fibers from the chains. In the chain formation step, the polymer molecules, in the aqueous solution, first interacted with each other to form hollow spheres; when the hollow spheres reached a critical size (typically larger than 2 μm as seen from SEM images), they started to aggregate and fuse into a pearl-necklace-like chain (Figure 2b). Subsequent outgrowth of longer fibers from the chain can be realized through the assembly of free polymer molecules in the solution onto the microspheres at the end of the pearl-necklace-like chains (Figure 2d), rather than through continuous attachment of microspheres, as there was a dramatic morphological difference between the chains (rough, Figure 2b and Supporting Information Figure S4-a) and outgrowing fibers (smooth, Figure 2d and Supporting Information Figure S4-b). However, the microspheres at the end of the chains might have been elongated first to facilitate the assembly of PVP molecules (Supporting Information, Figure S5). A continuous morphological transition from spherical particles into smooth fibers was observed at the interface of pearl-necklace-like chains and outgrowing fibers. With increasing distance from the central chains, the PVP hollow microspheres underwent the morphological change into ellipsoids, which are further elongated into rods and eventually smooth fibers. The hollow microspheres (Figure 2c) constituting the chains may eventually be fused into hollow fibers, which might be the same process of hollow nanoparticles fusing into nanotubes.[17] The branched character of the fibers was originated from the attachment of microspheres, which did not take part in the chain formation or was generated after the formation of the chain, onto the sidewall of outside fibers (Supporting Information, Figure S6). Once the attached microspheres were fused with long fibers (*i.e.*, stems), free polymer molecules in the solution would also assemble onto them, leading to the growth of a branch from the microspheres (Supporting Information, Figure S6).

The self-assembly behavior of PVP in the aqueous solution should be a general phenomenon, independent of their molecular weight. To prove this claim, we tried the same experiment with PVP of a higher molecular weight (40 kDa). Interestingly, same branched hollow structures were observed by SEM (Figure S7). However, the average diameter had been increased from 2−3 μm to around 5 μm. Such increase is reasonable because polymers with an increased polymer chain length may lead to a larger dimension of self-assembled microspheres and the consequent larger diameter of the resultant long fibers grown on the basis of the microspheres.

The formation of self-assembled branched hollow PVP fibers encouraged us to use them as a template to synthesize inorganic branched hollow fibers. Templating methods using chemical or biological templates

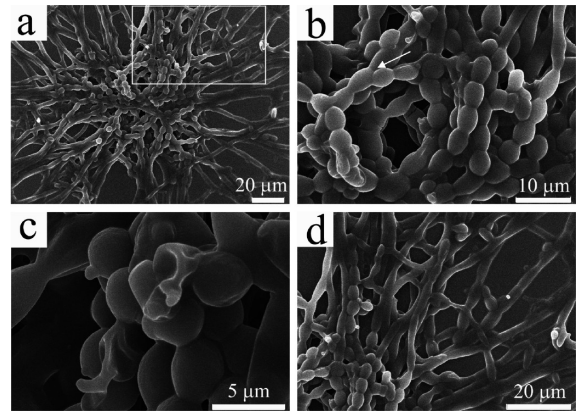

Figure 2. SEM images of PVP aggregates formed at the early stage: (a) an overall view of an aggregate with a core (made of pearl-necklace-like linear chains) from which all the fibers were grown; (b) a closer view of the core from the aggregate shown in panel a, highlighting that the formation and fusion of PVP microspheres into pearl-necklace-like chains (it should be noted that the branched structures are found in the core, as indicated by the arrow); (c) the pearl-necklace-like chains with some broken microspheres highlighting the hollow nature of PVP microspheres; (d) a closer view of the area highlighted by a white square highlighted in panel a, showing that free PVP molecules in the aqueous solutions continued to assemble onto the microspheres at the end of the pearl-necklace-like chains, and finally resulted in the formation of jellyfish-like large aggregate.

have been actively used in the synthesis of various nanomaterials, including nanowires,[30,31] nanotubes,[32−34] and hollow spheres,[35] and in the ordering of nanoparticles.[36] The idea is that a molecule or material with a high affinity to PVP, when added to the branched hollow PVP fiber networks in the suspension, should attach to the walls of networked PVP fibers and form a uniform coating layer, which will result in the replication of branched hollow fibrous PVP structure. Silica was chosen for this attempt for two reasons: first, silica is a biocompatible biomineral existing in many mineralized biological systems,[37] and thus the synthesis of branched hollow silica fibers may find application in biomedicine; second, silica is known to have strong hydrogen-bonding interaction with PVP[38] and silica formation on PVP-coated nanoparticles has been demonstrated in the synthesis of core/shell nanoparticles[39] and core/sheath nanowires.[40]

The self-assembled fibrous PVP structure was stable, with no visible destruction of the jellyfish-like bulk structure, when transferred from pure aqueous to ethanol aqueous solution (see experimental section). After silica deposition on the hollow PVP fibers, the mechanical strength of self-assembled PVP structures was enhanced, which was evidenced by significantly reduced collapse of the structures upon drying on the mica substrate. Also, unlike pure PVP hollow fibers in the semitransparent film, silica-coated PVP fibers appeared as a large white aggregate on mica. As shown in Figure 3a, large bundles of silica fibers were produced by using self-assembled branched PVP fibers as templates. In

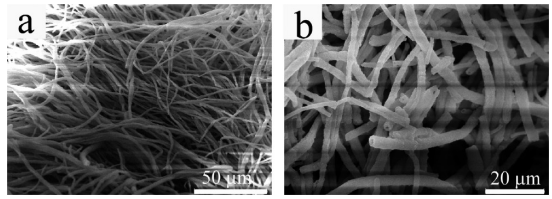

Figure 3. SEM images of silica fibers formed by silica deposition on the branched hollow PVP fibers shown in Figure 1: (a) bundles of silica fibers; (b) higher magnification showing that these fibers are hollow. The branched structures of individual fibers are not obvious because of the close packing of the branched fibers.

contrast to PVP fibers in Figure 1, most silica fibers maintained their cylindrical morphology, which is consistent with the above observation that the silica-coated PVP fibers had a much less structural collapse than the self-assembled pure PVP fibers when transferred from a solution phase to a solid substrate. The hollow character of PVP fibers was also duplicated by the silica fibers due to the formation of silica on the hollow PVP fiber surface (Figure 3b). Our investigation on the growth mechanism of silica onto PVP fibers demonstrated that the silica coating was actually occurring simultaneously on both outer and inner walls of the PVP fibers, though the silica growth rate on the outside surface might be faster than on the inner surface as the diffusion of the precursor to the outside surface is easier. This was evidenced directly from the fact that when the concentration of the silica precursor (TEOS) was increased, solid fibers without hollow channels were observed, suggesting the complete occupation of silica in the hollow channels due to silica deposition on the inner wall of the PVP fibers.

The silica fibers in Figure 3 are closely packed, which prevents us from visualizing the actual branched structure easily. So the sample shown in Figure 3 was treated with ultrasound in order to break up the bundles into individual fibers for verifying the branched structures of the silica fibers by SEM (see Experimental Section). It turned out that the branched nature was ubiquitous for long fibers. Figure 4a showed a typical image of branched long silica fibers. A three-branched fiber and a two-branched one are highlighted by arrows in the image. The angles between branches and main fiber axes were not fixed, but almost exclusively fell into a range of 45°∼90° (Figures 4b−f). This is of dramatic difference from the branched polyaniline and carbon nanotubes, in which angles between the branches and stems were all less than 45°.[15,16] Nonbranched fibers were also observed when the fibers were short, which indicates that they might be derived from the breaking of branched long fibers at the connection point between the branches and the stems. It should be noted that some nonfibrous silica products and flat fibers (Figure 4b) also exist on the mica substrate but they are very uncommon. They might arise from the negative effect of ultrasound, which caused the detachment of silica from some fibers and further disassociation of the fibers into tiny particles.

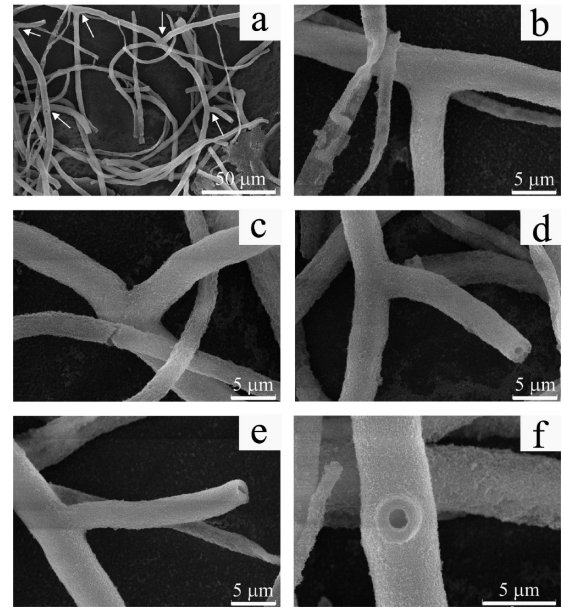

Figure 4. SEM images of individual silica fibers separated from the samples shown in Figure 3 by sonication: (a) low magnification image showing two branched fibers; (b−d) higher magnification of three branches of the fiber in upper center of image shown in image a; (e, f) higher magnification of two branches of the fiber on the left side of image shown in image a. Branches are indicated by arrows in image a.

Although direct templating of the preformed self-assembled fibrous PVP structures can produce nice branched hollow fibers, unlike silica, most materials do not have such strong interaction with PVP in the solution phase. For example, in an attempt to use the branched hollow PVP fibers as a template to form gold, $HAuCl_4$ was added to the PVP fibers and reduced with either sodium citrate or $NaBH_4$. However, no gold was formed on the inner or outer walls of the PVP fibers. To take advantage of the self-assembly of PVP and extend the use of the self-assembled PVP structures as a universal template for synthesizing branched hollow fibers, self-assembly of PVP-coated nanoparticles was adopted as an alternative. We hypothesize that PVP-coated nanoparticles, when dissolved in PVP solution, will coassemble with the free PVP molecules to form branched hollow fibers with the nanoparticles embedded in the solid walls of the fibers. Generally, in the coassembly of nanoparticles with PVP, the surface coat of the presynthesized nanoparticles (which could be any type of inorganic nanoparticles) was ligand replaced by PVP and the resultant PVP-coated nanoparticles were redispersed into a PVP aqueous solution (typically 5.7 wt % in this work). Since PVP can self-assemble to form a network of microfibers (Figure 1), PVP in the PVP-coated nanoparticles and the free PVP in the solution will co-self-assemble to form branched fibers due to the inherent self-assembly behavior of PVP.

Gold nanoparticles were used as a model to demonstrate the coassembly process. The PVP-coated gold

nanoparticles were prepared by following a reported procedure.[39] The self-assembled structure formed through the co-self-assembly of the PVP-coated gold nanoparticles and the free PVP in the solution was similar to that in the case of only PVP, but it was black (Supporting Information, Figure S1-b) when in solution and golden in color when dried on silicon wafer. As shown in Figure 5, gold fibers were very similar to the PVP microfibers shown in Figure 1 in terms of hollow and branched character, indicating that they were formed under a similar self-assembly mechanism. The energy dispersive X-ray spectrum (EDS) (Figure 5d) showed an intensive peak corresponding to gold. (The highest silicon peak was from the silicon wafer substrate; due to the limitation of X-ray detector used in our work, only elements beyond oxygen can be detected, so PVP was "invisible" under EDS.)

We found that the original gold nanoparticles solution was wine red in color, whereas the fibrous PVP-gold aggregate showed a black color (Supporting Information, Figure S1-b). So we believe that the gold nanoparticles in the fibers are in close proximity, which will lead to strong plasmon coupling between neighboring nanoparticles.[41] To further confirm this, we sonicated the PVP-gold aggregate for 15 min. After this treatment, the remaining visible aggregate was discarded and a TEM sample was prepared from the solution containing fiber debris. As can be seen from Figure 6a, the fibers are still composed of nanosized gold particles. Therefore, the black color of the PVP-gold aggregates must have arisen from the close packing of nanoparticles. Further evidence could also be found directly from the end of a broken fiber where only a few layers of gold nanoparticles were left (Figure 6b) and from debris that were stripped from the fiber sidewalls (Figure 6c). In addition, when the concentration of gold nanoparticles was decreased by 5 times, we could only obtain a red-colored jelly fish like PVP-gold aggregate, which was of the same color as the initial nanoparticle solution (Supporting Information, Figure S1-c; Figure S8). This fact is consistent with the explanation given above. Namely, a lower concentration of gold nanoparticles increased interparticle spacing of gold nanoparticles in the PVP fibers, which further weakened or canceled the plasmon coupling between nanoparticles.[42]

To investigate whether gold can form a fibrous structure when PVP matrix was damaged, PVP-gold fibers shown in Figure 5 were treated in an oven at 220 °C for 24 h, which was far above the glass transition temperature of the polymer. Under this condition, pure self-assembled fibrous PVP structure was found to be completely deformed into a continuous film without any fibrous character. A polymer film was also observed after heating the gold fibers, indicating that there was phase separation of melted PVP matrix from gold. Nevertheless, the main structure of gold fibers was intact. As shown in Figure 7a, hollow character was maintained in almost all the fibers, although they were slightly collapsed from cylindrical into elliptical shape. A significant difference was seen at a higher magnification. Before

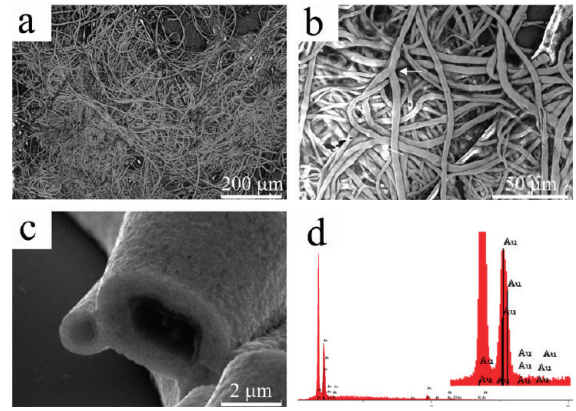

Figure 5. SEM images of hollow gold fibers formed throught the co-self-assembly of PVP-coated gold nanoparticles with free PVP in a solution: (a) low magnification; (b) higher magnification showing the branched nature of fibers (branches are indicated by arrows); (c) higher magnification of the tip of the fibers showing that the fibers are hollow and have smooth cross section; (d) EDS spectrum showing the existence of gold in the fibers (inset is an amplification of the gold peak, the highest peak is from silicon substrate).

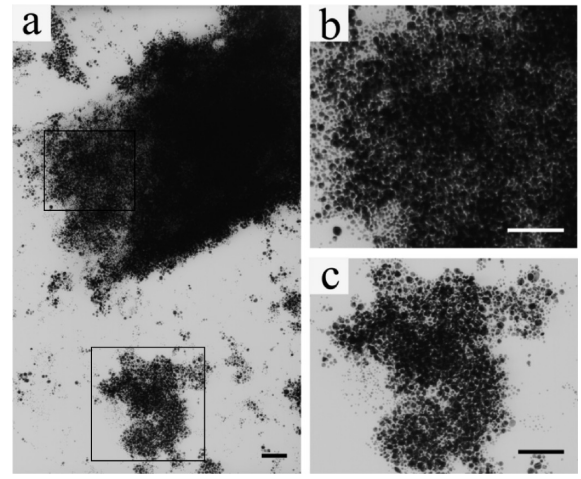

Figure 6. TEM images of debris of PVP-gold fibers after the fibers were sonicated for 15 min: (a) the fibers were still composed of nanosized gold particles, which were not fused into larger particles; (b, c) higher magnification showing dense packing of gold nanoparticles in the fibers highlighted by a square in top left and bottom, respectively. The gold aggregate shown in the bottom in image a was detached from the PVP-gold fibers due to sonication. All scale bars are 200 nm.

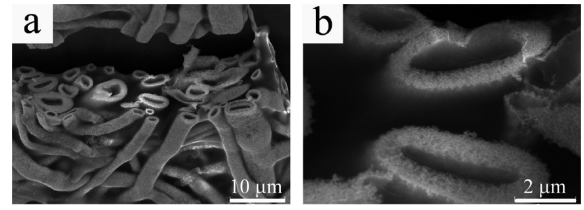

Figure 7. SEM images of gold fibers that have been treated in the oven at 220 °C for 24 h: (a) fiber structure is not destroyed by heating upon the glass transition temperature of PVP; (b) after PVP has been melted away, the cross sections of the fibers become porous.

heating, the gold-PVP fibers had a smooth cross section (Figure 5c), which became porous after heating (Figure 7b). On the basis of the above observations, it is reasonable to conclude that (1) PVP-coated nanoparticles coassemble with PVP to form branched hollow fibers in the solution phase; (2) in the as-prepared gold fibers, gold nanoparticles had a very high density in the PVP matrix; and (3) upon heating above the glass transition temperature of PVP, PVP is gradually melted away, and meanwhile, gold nanoparticles are fused together to form porous fibers.

CONCLUSIONS

Jellyfish-like self-assembled fibrous PVP structure was observed after a relative long-term aging of PVP solution under room temperature. By directly templating the formation of silica on the self-assembled fibrous PVP structure, branched hollow silica fibers were synthesized for the first time. To demonstrate that PVP can be potentially employed as a universal template to prepare branched hollow fibers of various materials, branched hollow gold fibers were synthesized from PVP-coated gold nanoparticles through the synergistic self-assembly of PVP-coated gold nanoparticles and the free PVP molecules in the solution phase. The gold fibers were structurally stable when heated above the glass transition temperature of the polymer. The branched fibers produced in this work may serve as new templates for the synthesis of fibers or tubes of other materials.

EXPERIMENTAL SECTION

Formation of Self-Assembled Hollow Fibrous PVP Structures. In a 15-ml vial, 600 mg of PVP (10 kg/mol) was dissolved into 10 mL of distilled water (PVP 5.7 wt %). The solution was then sonicated for 10 min to ensure homogeneous distribution of the polymer. After this step, the vial was capped and the solution was placed on the benchtop at room temperature for about 2 weeks. During this period of time, tiny polymeric aggregates were found at the bottom of the vial in one week and slowly grew larger and larger in the following week.

Growth of Silica on Self-Assembled Hollow Fibrous PVP Structures. The polymer aggregate made of self-assembled hollow PVP fibers was transferred to a 5-ml vial by Pasteur pipet and washed with distilled water twice to remove free polymer in the solution. The aggregate was then suspended in a 1 mL of ethanol aqueous solution (ethanol/water = 4:1 v/v). To the resultant suspension were added 50 μL of tetraethoxysilane (TEOS) and 50 μL of NH_4OH. The suspension was further mixed by gently inverting the vial for several times. To form a uniform silica layer onto the polymer aggregate, during the reaction, the vial was placed onto an aliquot mixer rocker for about 2 h. The as-grown silica microfibers were washed twice with ethanol to get rid of the products that might be formed in the hydrolysis reaction other than the silica microfibers.

Formation of Hollow Gold Fibers by Co-self-assembly of PVP-Coated Gold Nanoparticles and Free PVP Molecules. Gold nanoparticles were synthesized through the reduction of gold chloride ($HAuCl_4$) by sodium citrate. The synthesis system included 5 mL of 5.9 mM $HAuCl_4$, 3 mL of 38.8 mM sodium citrate and 42 mL of distilled water. Ligand replacement of citrate ions by PVP on the surface of gold nanoparticles was carried out according to the procedure reported in the literature.[39] 50 mL of PVP-stabilized gold nanoparticles were centrifuged and redispersed into 10 mL (Supporting Infomation, Figure S1b) or 50 mL (Figure S1c) of PVP aqueous solution (PVP 5.7 wt %). The mixture was then allowed to stay on the benchtop at room temperature for 2 weeks. Gold microfibers were formed through the coassembly of the PVP-coated gold nanoparticles and PVP.

Characterization. Silica and gold microfibers were characterized by scanning electron microscope (SEM) JEOL 880 at 15 kV in both bundled and individual fibers. The bundles of fibers were prepared by directly placing a bulk piece of as-synthesized silica onto a piece of freshly cleaved mica. Individual fibers were prepared by sonicating the bundles for 2−3 min, and then by casting a drop of suspension onto mica. Gold microfibers were prepared in the same way, except that instead of using mica, silicon wafer was employed as a substrate. Samples of silica were coated with a thin layer of gold platinum by sputter-coating prior to SEM imaging; whereas gold microfibers samples were directly subjected to SEM examination without any additional coating.

Acknowledgment. We thank the National Science Foundation, National Institutes of Health, Department of Defense Congressionally Directed Medical Research Programs, and the Oklahoma Center for the Advancement of Science and Technology for financial support.

Supporting Information Available: Photographs of jellyfish like structures, TEM image of hollow fibers, dynamic light scattering data demonstrating the polymer aggregate size change during aging of PVP solution, optical microscope images of fibers at early and late stages, SEM images showing the formation of fibers at early stage, with different nanoparticle concentration, and with PVP of a different molecular weight. This material is available free of charge *via* the Internet at http://pubs.acs.org.

REFERENCES AND NOTES

1. Lei, F. M.; Qu, Y. H.; Gan, Y. L.; Gebauer, A.; Kaiser, M. The Feather Microstructure of Passerine Sparrows in China. *J. Ornithol.* **2002**, *143*, 205–212.
2. Dyck, J. The Evolution of Feathers. *Zool. Scr.* **1985**, *14*, 137–154.
3. Whitesides, G. M. The Origins and the Future of Microfluidics. *Nature* **2006**, *442*, 368–373.
4. Borenstein, J. T.; Weinberg, E. J.; Orrick, B. K.; Sundback, C.; Kaazempur-Mofrad, M. R.; Vacanti, J. P. Microfabrication of Three-Dimensional Engineered Scaffolds. *Tissue Eng.* **2007**, *13*, 1837–1844.
5. Zhang, W. J.; Liu, W.; Cui, L.; Cao, Y. L. Tissue Engineering of Blood Vessel. *J. Cell. Mol. Med.* **2007**, *11*, 945–957.
6. Huh, D.; Fujioka, H.; Tung, Y. C.; Futai, N.; Paine, R.; Grotberg, J. B.; Takayama, S. Acoustically Detectable Cellular-Level Lung Injury Induced by Fluid Mechanical Stresses in Microfluidic Airway Systems. *Proc. Natl. Acad. Sci. U.S.A.* **2007**, *104*, 18886–18891.
7. Lin, Y. M.; Boccaccini, A. R.; Polak, J. M.; Bishop, A. E. Biocompatibility of Poly-DL-lactic Acid (PDLLA) for Lung Tissue Engineering. *J. Biomater. Appl.* **2006**, *21*, 109–118.
8. Zhang, H. X.; Ge, J. P.; Wang, J.; Li, Y. D. Atmospheric Pressure Chemical Vapour Deposition Synthesis of Sulfides, Oxides, Silicides and Metal Nanowires with Metal Chloride Precursors. *Nanotechnology* **2006**, *17*, S253–S261.
9. Ando, Y.; Zhao, X.; Sugai, T.; Kumar, M. Growing Carbon Nanotubes. *Mater. Today* **2004**, *7*, 22–29.
10. Colli, A.; Hofmann, S.; Fasoli, A.; Ferrari, A. C.; Ducati, C.; Dunin-Borkowski, R. E.; Robertson, J. Synthesis and Optical Properties of Silicon Nanowires Grown by Different Methods. *Appl. Phys. A: Mater. Sci. Process.* **2006**, *85*, 247–253.
11. Cao, G. Z.; Liu, D. W. Template-Based Synthesis of Nanorod, Nanowire, and Nanotube Arrays. *Adv. Colloid Interf. Sci.* **2008**, *136*, 45–64.

12. Li, D.; Xia, Y. N. Electrospinning of Nanofibers: Reinventing the Wheel. *Adv. Mater.* **2004**, *16*, 1151–1170.
13. Zhao, Y.; Cao, X. Y.; Jiang, L. Bio-mimic Multichannel Microtubes by a Facile Method. *J. Am. Chem. Soc.* **2007**, *129*, 764–765.
14. Xia, Y. N.; Yang, P. D.; Sun, Y. G.; Wu, Y. Y.; Mayers, B.; Gates, B.; Yin, Y. D.; Kim, F.; Yan, Y. Q. One-Dimensional Nanostructures: Synthesis, Characterization, And Applications. *Adv. Mater.* **2003**, *15*, 353–389.
15. Meng, G. W.; Jung, Y. J.; Cao, A. Y.; Vajtai, R.; Ajayan, P. M. Controlled Fabrication of Hierarchically Branched Nanopores, Nanotubes, And Nanowires. *Proc. Natl. Acad. Sci. U.S.A.* **2005**, *102*, 7074–7078.
16. Li, J.; Papadopoulos, C.; Xu, J. Nanoelectronics—Growing Y-Junction Carbon Nanotubes. *Nature* **1999**, *402*, 253–254.
17. Wei, Z. X.; Zhang, L. J.; Yu, M.; Yang, Y. S.; Wan, M. X. Self-Assembling Submicrometer-Sized Tube Junctions and Dendrites of Conducting Polymers. *Adv. Mater.* **2003**, *15*, 1382+.
18. Xiong, Y. J.; Xia, Y. N. Shape-Controlled Synthesis of Metal Nanostructures: The Case of Palladium. *Adv. Mater.* **2007**, *19*, 3385–3391.
19. Wiley, B.; Sun, Y. G.; Mayers, B.; Xia, Y. N. Shape-Controlled Synthesis of Metal Nanostructures: The Case of Silver. *Chem.—Eur. J.* **2005**, *11*, 454–463.
20. Xia, Y. N.; Xiong, Y. J.; Lim, B.; Skrabalak, S., E. Shape-Controlled Synthesis of Metal Nanocrystals: Simple Chemistry Meets Complex Physics. *Angew. Chem., Int. Ed.* **2009**, *48*, 60–103.
21. Sun, Y. G.; Mayers, B.; Herricks, T.; Xia, Y. N. Polyol Synthesis of Uniform Silver Nanowires: A Plausible Growth Mechanism and the Supporting Evidence. *Nano Lett.* **2003**, *3*, 955–960.
22. Kang, J. S.; Kim, K. Y.; Lee, Y. M. Preparation of PVP Immobilized Microporous Chlorinated Polyvinyl Chloride Membranes on Fabric and Their Hydraulic Permeation Behavior. *J. Membr. Sci.* **2003**, *214*, 311–321.
23. Hayama, M.; Yamamoto, K.; Kohori, F.; Sakai, K. How Polysulfone Dialysis Membranes Containing Polyvinylpyrrolidone Achieve Excellent Biocompatibility. *J. Membr. Sci.* **2004**, *234*, 41–49.
24. Ochoa, N. A.; Pradanos, P.; Palacio, L.; Pagliero, C.; Marchese, J.; Hernandez, A. Pore Size Distributions Based on AFM Imaging and Retention of Multidisperse Polymer Solutes—Characterisation of Polyethersulfone UF Membranes with Dopes Containing Different PVP. *J. Membr. Sci.* **2001**, *187*, 227–237.
25. Han, M. J.; Nam, S. T. Thermodynamic and Rheological Variation in Polysulfone Solution by PVP and Its Effect in the Preparation of Phase Inversion Membrane. *J. Membr. Sci.* **2002**, *202*, 55–61.
26. Guven, O.; Eltan, E. Molecular Association in Aqueous-Solutions of High Molecular-Weight Poly(*N*-vinyl-2-pyrrolidone). *Makromol. Chem., Macromol. Chem. Phys.* **1981**, *182*, 3129–3134.
27. Guven, O.; Yigit, F. Hydrophilic and Hydrophobic Interactions in Alcohol-Solutions of High Molecular-Weight Poly(*N*-vinyl-2-pyrrolidone). *Colloid Polym. Sci.* **1984**, *262*, 892–895.
28. Sun, T.; King, H. E. Aggregation Behavior in the Semidilute Poly(*N*-vinyl-2-pyrrolidone)/Water System. *Macromolecules* **1996**, *29*, 3175–3181.
29. Itakura, M.; Inomata, K.; Nose, T. Aggregation Behavior of Poly(*N*,*N*-diethylacrylamide) in Aqueous Solution. *Polymer* **2000**, *41*, 8681–8687.
30. Mao, C. B.; Solis, D. J.; Reiss, B. D.; Kottmann, S. T.; Sweeney, R. Y.; Hayhurst, A.; Georgiou, G.; Iverson, B.; Belcher, A. M. Virus-Based Toolkit for the Directed Synthesis of Magnetic and Semiconducting Nanowires. *Science* **2004**, *303*, 213–217.
31. Nam, K. T.; Kim, D. W.; Yoo, P. J.; Chiang, C. Y.; Meethong, N.; Hammond, P. T.; Chiang, Y. M.; Belcher, A. M. Virus-Enabled Synthesis and Assembly of Nanowires for Lithium Ion Battery Electrodes. *Science* **2006**, *312*, 885–888.
32. Shenton, W.; Douglas, T.; Young, M.; Stubbs, G.; Mann, S. Inorganic−Organic Nanotube Composites from Template Mineralization of Tobacco Mosaic Virus. *Adv. Mater.* **1999**, *11*, 253+.
33. Niu, Z.; Liu, J.; Lee, L. A.; Bruckman, M. A.; Zhao, D.; Koley, G.; Wang, Q. Biological Templated Synthesis of Water-Soluble Conductive Polymeric Nanowires. *Nano Lett.* **2007**, *7*, 3729–3733.
34. Wang, F. K.; Li, D.; Mao, C. B. Genetically Modifiable Flagella as Templates for Silica Fibers: From Hybrid Nanotubes to 1D Periodic Nanohole Arrays. *Adv. Funct. Mater.* **2008**, *18*, 4007–4013.
35. Caruso, F.; Caruso, R. A.; Mohwald, H. Nanoengineering of Inorganic and Hybrid Hollow Spheres by Colloidal Templating. *Science* **1998**, *282*, 1111–1114.
36. McMillan, R. A.; Paavola, C. D.; Howard, J.; Chan, S. L.; Zaluzec, N. J.; Trent, J. D. Ordered Nanoparticle Arrays Formed on Engineered Chaperonin Protein Templates. *Nat. Mater.* **2002**, *1*, 247–252.
37. Foo, C. W. P.; Patwardhan, S. V.; Belton, D. J.; Kitchel, B.; Anastasiades, D.; Huang, J.; Naik, R. R.; Perry, C. C.; Kaplan, D. L. Novel Nanocomposites from Spider Silk-Silica Fusion (Chimeric) Proteins. *Proc. Natl. Acad. Sci. U.S.A.* **2006**, *103*, 9428–9433.
38. Toki, M.; Chow, T. Y.; Ohnaka, T.; Samura, H.; Saegusa, T. Structure of Poly(vinylpyrrolidone)−Silica Hybrid. *Polym. Bull.* **1992**, *29*, 653–660.
39. Graf, C.; Vossen, D. L. J.; Imhof, A.; van Blaaderen, A. A General Method to Coat Colloidal Particles with Silica. *Langmuir* **2003**, *19*, 6693–6700.
40. Yin, Y. D.; Lu, Y.; Sun, Y. G.; Xia, Y. N. Silver Nanowires Can Be Directly Coated with Amorphous Silica To Generate Well-Controlled Coaxial Nanocables of Silver/Silica. *Nano Lett.* **2002**, *2*, 427–430.
41. Ghosh, S. K.; Pal, T. Interparticle Coupling Effect on the Surface Plasmon Resonance of Gold Nanoparticles: From Theory to Applications. *Chem. Rev.* **2007**, *107*, 4797–4862.
42. Moskovits, M. Surface-Enhanced Raman Spectroscopy: A Brief Retrospective. *J. Raman Spectrosc.* **2005**, *36*, 485–496.